Machine learning guided discovery of Non-Linear Optical materials

Sownyak Mondal* and Raheel Hammad*

Tata Institute of Fundamental Research Hyderabad, Hyderabad-500046*, Telangana, India.*

E-mail: msownyak@tifrh.res.in; raheelhammad@tifrh.res.in

Abstract

Nonlinear optical(NLO) materials are crucial in achieving desired frequencies in solid-state lasers. So far, new NLO materials have been discovered using high-throughput calculations or chemical intuition. This study demonstrates the effectiveness of utilizing a high refractive index as a proxy for a high second harmonic generation(SHG) coefficient. We also emphasize the importance of hardness in screening balanced NLO materials. We develop two machine learning models to predict refractive indices and Vickers hardness. By applying these models to the OQMD database, we identify potential NLO candidates based on non-centrosymmetricity, refractive index, hardness value, and bandgap properties. Our findings are validated using density functional theory(DFT) calculations. Notably, our approach successfully identifies several already established NLO materials, reinforcing the validity of our methodology.

Introduction

Non-linear optical(NLO) materials are a special class of materials that exhibit anisotropic properties under electromagnetic radiation.[1] These NLO materials are crucial in achieving desired frequencies in all solid state lasers that are utilized widely in various applica-

tions like remote communications, formation of entangled photon pairs, medical diagnosis, etc.[2–5] To date, only a handful of NLO materials have been discovered and utilized, including KBe2BO3F2 (KBBF),[6] β-BaB2O4,[7] KH2PO4 (KDP),[8] KTiOPO4,[9] AgGaS2,[10] and KTiOPO4 (KTP).[11] Several studies have shown that sulfide plays a crucial role in developing mid-far infrared nonlinear optical materials.[2,12–14] A practical NLO material must have i) Large second-harmonic generation (SHG) coefficient ($\chi(2)$) value, preferably greater than 3.9 pmV^{-1},[15] to ensure efficient frequency conversion. ii) moderate to high band gap (>1.5-2.0 eV),[16] to have high laser-induced damage thresholds (LIDTs). Qingchen Wu et al. explained why an NLO material must have a high thermal conductivity which in turn leads to high LIDT.[15] However, a highly intense laser beam can induce rapid heating, not only causing localized thermal expansion but also non-uniform stress distribution which can lead to deformation, cracking, etc. Additionally, previous studies have shown the importance of Vickers hardness for NLO materials,[17,18] Therefore we choose a cutoff with a hardness value($>$ 20 GPa) based on the distribution of hardness(Figure S3) to screen materials. So far, high-throughput screening techniques based on intuition have proven successful in the discovery of new specialized materials such as NLO and auxetic materials.[6,19–22] However, high throughput is often time-consuming, computationally intensive, and cumbersome due to the large amount of data processing required.

In recent years, the combination of abundant data from computational and experimental methods, along with advanced machine learning (ML) techniques, has propelled materials science into a new era, often called the fourth paradigm of scientific exploration.[23] ML algorithms are now widely used to predict the mechanical and electronic properties of materials with greater efficiency and accuracy.[24–26] Zhang et al. proposed a novel approach using multilevel descriptors for the ML-assisted screening of inorganic NLO crystals.[27] ML models have been developed to predict the symmetry type of crystals and discover new non-centrosymmetric materials.[28] To our knowledge, there exists only a single ML model based on few data points to predict NLO coefficient.[29] This limitation arises due to the absence of

an existing database specific to this property.

In this study, we first explain why a high refractive index can serve as a proxy for a high SHG coefficient. Subsequently, we construct a machine learning model to predict materials with high refractive index. To enhance the robustness and accuracy of our model, we take assistance from existing empirical relationships between band gap and refractive index. Additionally, we develop another regression model to forecast Vickers hardness values. Following the establishment of these models, we apply them to all non-centrosymmetric materials within the OQMD database. Through this comprehensive screening process(figure 1), we identify potential candidates for high-performance NLO materials based on criteria such as high refractive index, bandgap, and hardness values. Unsurprisingly, our efforts produce several materials that have already been confirmed as effective NLO substances, highlighting the effectiveness of our approach.

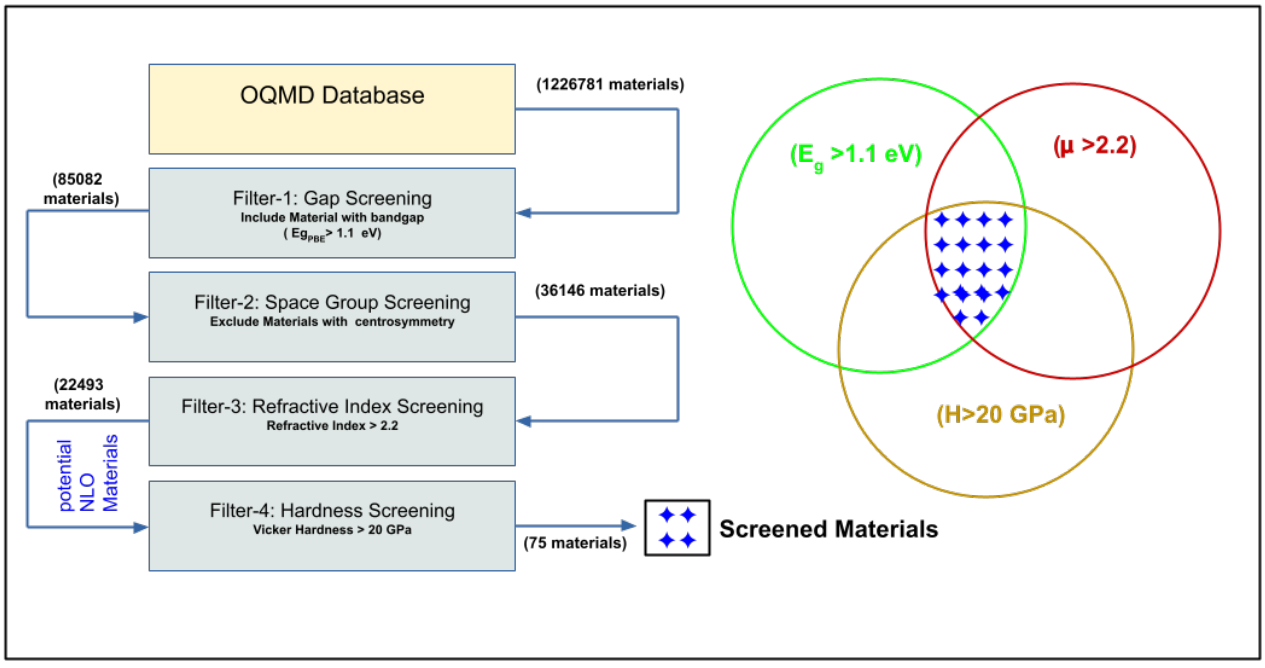

Figure 1: Demonstration of the full scheme to discover new NLO materials

Methods

Elastic and optical properties are computed using the Vienna ab initio Simulation Package (VASP) in projector augmented wave (PAW) mode, employing the generalized gradient approximation (GGA) with the Perdew-Burke-Ernzerhof (PBE) functional for exchange-correlation energy calculations.[30] We use the Materials Project workflow library called Atomate for computing both properties.[31] Initially, the crystal structures are relaxed to obtain structures in a state of approximately zero stress. Subsequently, perturbations are applied to the lattice vectors, and the resulting stress tensor is computed. From this tensor, aggregate properties such as Voigt bounds on the bulk and shear moduli are derived. Calculations of Optical properties involve an initial static calculation followed by a non-self-consistent field calculation with LOPTICS set. The static calculation is performed to determine if the material requires magnetism to be set and to establish the total number of bands. The non-self-consistent field calculation contains 1.3 times the number of bands obtained in the static calculation, as the highest bands are often not properly converged in VASP. This workflow enabled the computation of optical properties for the materials under study. The force and energy cutoff for relaxation and self-consistent field (SCF) cycles are taken to be 10^{-2} eV/$\mathring{A}$ and 10^{-7} eV respectively. This ensures the accuracy and reliability of the computed elastic constants and optical properties.

Results and discussion

Miller (1964) observed substantial variations in the values of the second-order susceptibility $\chi(2)$ among eleven different materials and discovered that $\chi(2)$ is directly proportional to the product of three linear susceptibilities.[32] This corroborates high refractive index materials potentially showing high response in the nonlinear regime. Jackson et al. showed a reduced

formula of Miller's rule in the limit of very high refractive index (μ) in equation 1.[33]

$$\chi(2) = 0.436 \times \mu^6 \tag{1}$$

Moreover, Jackson et al. compiled a table containing data extracted from various sources in the literature.[33] The graphical representation of the table is shown in Figure S1, which underscores the observed correlation between elevated refractive indices and higher values of the second-order NLO coefficient. All these findings collectively suggest that high refractive index values may serve as a reliable indicator (proxy) for predicting high nonlinear optical (NLO) coefficients. This correlation could potentially streamline the search for novel NLO materials, offering researchers a valuable shortcut.

ML Model for Refractive Index

The selection and engineering of features play a crucial role in the performance and interpretability of machine learning models, as they directly influence the model's ability to capture relevant patterns and relationships within the data. On the other hand, it has been of considerable interest to the scientific community to understand the relationship between refractive index and band gap. Various empirical formulas have been proposed in the literature to characterize this relationship.[34] Among the most widely cited are equations 3, 4, 5, and 6. In this study, we utilize the predicted refractive indices obtained from these formulas (μ_1,μ_2,μ_3 and μ_4) as features for our Machine Learning Model. For clarification, it is important to note that these values do not represent the actual refractive index of any specific material; rather, these are just features derived from those empirical formulas. The incorporation of these physics-based features has yielded notable enhancements to the model's performance when contrasted with existing methodologies. These formulas are (E_g is band gap):

Moss Formula:[35]

$$\mu^4 \times E_g = 95.0(eV) \tag{2}$$

Ravindra Formula:[36]

$$\mu = 4.084 - 0.62 \times E_g \tag{3}$$

Herve–Vandamme Formula:[37]

$$\mu^2 = 1 + \frac{13.6(eV)}{3.47(eV) + E_g} \tag{4}$$

Reddy Formula[38] :

$$\mu^4 \times (E_g - 0.365) = 154 \tag{5}$$

On top of these four physics-based features, we have added crystal properties and elemental properties as descriptors. The elemental descriptors are delineated through mathematical expressions, namely the average, minimum, maximum, and difference, respectively.

In the context of the present study, a dataset comprising 6588 data points[39] and initially encompassing 160 features was subjected to a Random Forest feature selection process. This method facilitated identifying and prioritizing the top 40 features based on their respective importance scores. The average metallic valence, average density, band gap, and four empirical μ_s(μ_1,μ_2,μ_3 and μ_4) are the top descriptors based on the importance scores. Given the observed redundancy within the empirical parameters of those empirical μ_s and bandgap, we have used μ_1 in the final model. We have showcased the Pearson correlation between the top features and refractive index in Figure S2. Additionally, this plot shows that the top features have low correlation with each other, which indicates low redundancy between features. In the evaluation of various machine learning algorithms for the prediction of refractive index, Gradient Boosting Regression emerged as the most proficient performer, showcasing superior predictive accuracy and robustness compared to alternative methods. We achieve a coefficient of determination (R^2) of 0.93 and mean absolute

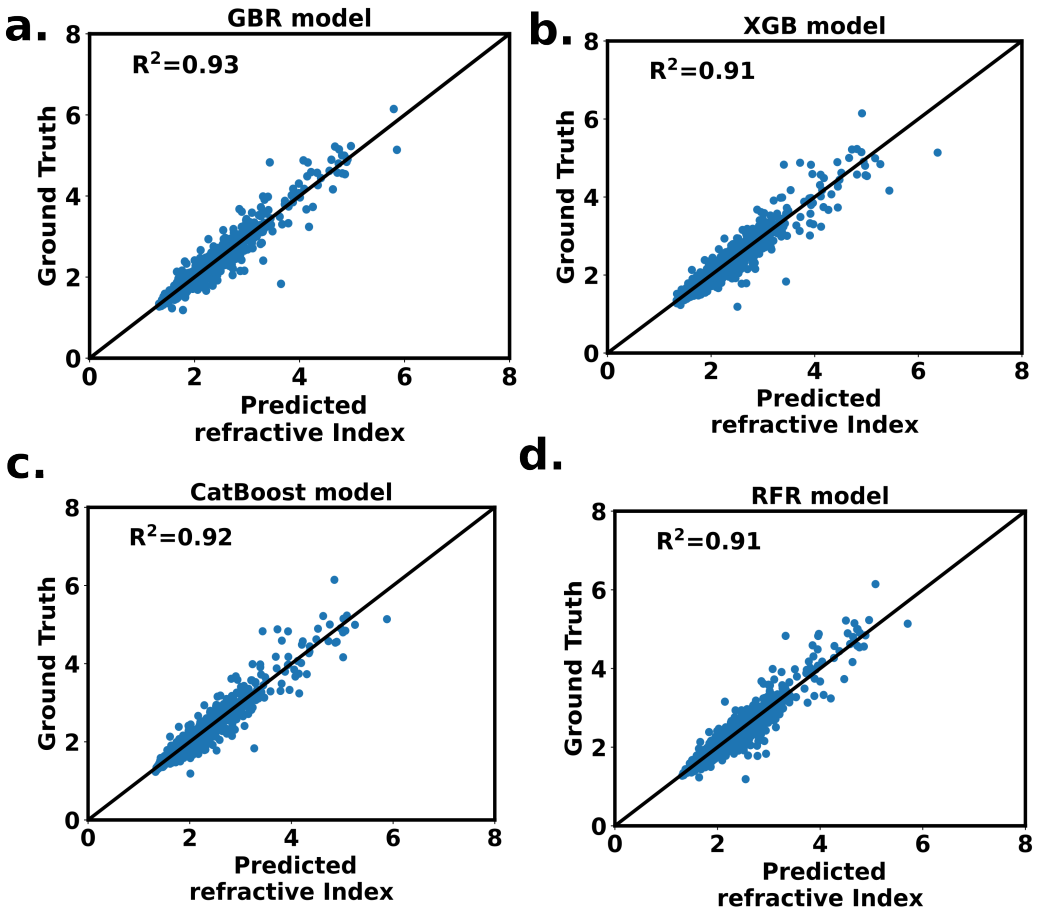

Figure 2: Performance of different algorithms for Refractive index prediction

error (MAE) of 0.11 markedly surpassing the performance metrics reported in the existing literature of refractive index prediction models. These results are obtained through the implementation of k-fold cross-validation, specifically employing a 5-fold validation approach, ensuring robustness against overfitting. Hyperparameter optimization is conducted using a grid search method, with the resulting hyperparameter configurations provided in `https://github.com/sownyak/ml_refractive_hardness`. Alternative methods including eXtreme Gradient Boosting (XGB), CatBoost, and Random Forest Regression (RFR) were also evaluated, yielding R^2 values of 0.91, 0.92, and 0.91, respectively. However, none of these approaches exhibited performance comparable to that of GBR.

ML Model for Superhard

In recent years, the research community has achieved notable strides in the development of resilient machine learning (ML) models for Superhard materials.[26,40] Bulk modulus(B) and

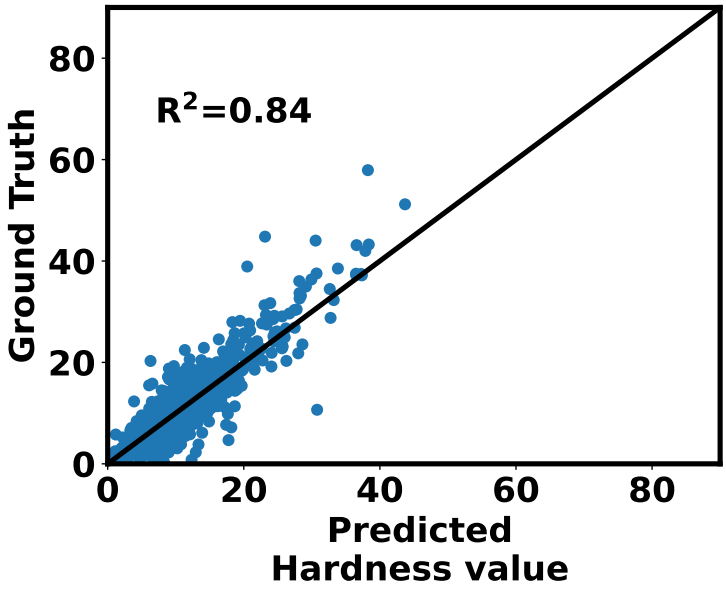

Figure 3: Catboost model for Vickers Hardness prediction

shear modulus(G) values, delineated in Voigt notation, have been systematically gathered from the Materials Project database. Subsequently, Equation 6 has been employed to compute the hardness parameter, thereby designated as the target quantity in our investigation.[41]

$$H = 2 \times \left(\frac{G^3}{B^2}\right)^{0.585} \tag{6}$$

Notably, the model's foundation rests upon data sourced from the Materials Project Database, comprising an array of salient features such as average crystal radius, average melting point (in Kelvin), maximum valence d, and volume, among others. We obtain a coefficient of determination (R^2) of 0.84 and a mean absolute error (MAE) of 2.21 GPa. Similar to the refractive index model, we used 5-fold validation to compute the metrics mentioned earlier.

Prediction Set

We have used the OQMD dataset to look for potential NLO materials .[42] This was done since the number of non-centrosymmetric materials in the OQMD database is ≈ 36,146 (having bandgap 1.1 eV) which is high. Although to have a higher Laser Induced Damage Threshold (LIDT) and to reduce spontaneous emission one needs a bandgap of $> 1.5 - 2.0$ eV,[16] here we have reduced the bandgap threshold considering the bandgap underestimation at PBE level. On top of that, OQMD database is relatively less explored in even high-throughput screening of NLO materials. Therefore we have featured these materials from OQMD via the same procedure used for the training set(Materials Project).

This was done since it is well-established in the literature that only non-centrosymmetric materials can have NLO properties. This attribute facilitates the modulation of electronic polarization under the influence of an electric field, thereby contributing significantly to the material's response to external stimuli and its suitability for NLO applications.

In the context of NLO materials, the relationship between band gap and NLO efficiency is crucial. A larger band gap is typically associated with a reduction in the SHG coefficient[33] , making it challenging to find materials with both high band gaps and strong NLO properties. Despite this, maintaining a lower cutoff of the band gap allows for the inclusion of semiconductors among potential NLO materials.

In pursuit of materials exhibiting exceptional optical and mechanical properties, our criteria entail setting a threshold refractive index of 2.2 and a minimum hardness value of 20.0 GPa

Following the criteria outlined in Figure (1), we screened a total of 36.2k non-centrosymmetric materials, afterward the refractive index criteria filters out low SHG coefficient materials and we are left with 22K potential NLO materials. 15 out of these materials have SHG coefficients available in literature[29] , indeed all of them have very high SHG coefficients and correspondingly high refractive index (Table S1) ultimately identifying 75 as desirable can-

Table 1: List of screened materials, C stands for DFT computed while O stands for collected from OQMD

Calculation Id(O)	Chemical Formula(O)	Spacegroup(O)	refractive index(C)	Hardness(C)	Band G
10258	B1 C2 N1	Pmm2	2.438	76.69	1.878
10317	Be1 N1 P1 Si1	P-4m2	3.175	34.5	1.139
30006	Be1 N2 Si1	I-42d	2.194	33.33	3.673
30132	B1 C2 N1	P2221	2.417	78.37	2.374
1290316	Be1 C1 P2	I-42d	2.769	19.78	1.366
3125179	Be1 Ge1 N2	I-42d	3.35	26.83	3.508
3125183	Be1 Ge1 N2	I-42d	2.37	27.97	3.714
3125237	Mg1 N2 W1	P-6m2	2.194	33.33	1.376
4296785	B1 Ga3 N4	P-43m	2.619	25.83	2.632
4297031	B3 Ga1 N4	P-43m	3.026	21.87	3.853
4297032	Al3 B1 N4	P-43m	3.247	19.33	3.459
4499927	Al1 B3 N4	P-43m	2.288	23.41	3.755
4515690	Al3 Ga1 N4	P-43m	2.219	33.31	3.532
4642269	B6 C1 Na1	Amm2	2.793	39.04	1.619
4920840	Al5 C3 N1	P63mc	3.36	32.87	1.519
5096941	Li1 Mg1 N1	F-43m	2.295	23.45	2.784
5139850	Li1 Mg1 N1	F-43m	2.473	22.61	2.573
5139851	Be2 N3 P1	Cmc21	2.274	37.09	4.989
5139853	Be2 N3 P1 Si2	C2	2.255	24.26	1.398
5139858	Be1 N1 P1 Si1	Cc	2.21	37.89	1.395
5139865	Be2 N1 P3 Si2	C2	2.262	20.56	1.242

didates. From this pool, we randomly selected 20 materials and conducted first-principles calculations to evaluate their optical and mechanical properties. **These computational results closely align with the values predicted by our machine learning models**. Subsequent literature review revealed that certain materials, such as boron-substituted aluminum nitride[43] indeed demonstrate non-linear optical characteristics. The DFT computed properties of these 20 materials have been shown in Table(1). All the codes are freely available in GitHub (`https://github.com/sownyak/ml_refractive_hardness`)

Conclusion

In summary, our study demonstrates the effectiveness of using a high refractive index as a proxy for a high SHG coefficient. We develop two separate ML models: one for predicting high refractive indices and another for Vickers hardness. Subsequently, we identify potential NLO materials from the largely unexplored OQMD database, focusing on properties such as non-centrosymmetricity, high refractive index, hardness value, and bandgap.

Furthermore, we validate our findings by employing density functional theory(DFT) calculations to validate the ML-predicted refractive indices and hardness values. It is important to acknowledge a limitation of our approach, namely the inability to calculate SHG coefficients due to resource constraints directly. However, despite this limitation, several materials identified in our study have already been established as effective NLO substances in existing literature. We believe that the identified materials hold promise as potential NLO candidates.

Overall, our approach of using a proxy to discover special class of materials is quite general and it can be extrapolated to various other contexts.

Acknowledgement

The authors thank Prof. Soumya Ghosh for the computing facility and the critical comments on the manuscript. They are also grateful to Chandrashekhar Iyer and Prof. Chaitanya Kumar Suddapalli for useful discussions. They acknowledge TIFR Hyderabad for funding and facilities.

References

(1) Arivuoli, D. Fundamentals of nonlinear optical materials. *Pramana* **2001**, *57*, 871–883.

(2) Li, Y.; Luo, J.; Zhao, S. Local polarity-induced assembly of second-order nonlinear optical materials. *Accounts of Chemical Research* **2022**, *55*, 3460–3469.

(3) Liang, F.; Kang, L.; Lin, Z.; Wu, Y.; Chen, C. Analysis and prediction of mid-IR nonlinear optical metal sulfides with diamond-like structures. *Coordination Chemistry Reviews* **2017**, *333*, 57–70.

(4) Wang, Y.; Pan, S. Recent development of metal borate halides: Crystal chemistry and application in second-order NLO materials. *Coordination Chemistry Reviews* **2016**, *323*, 15–35.

(5) Liu, X.; Gong, P.; Yang, Y.; Song, G.; Lin, Z. Nitrate nonlinear optical crystals: A survey on structure-performance relationships. *Coordination Chemistry Reviews* **2019**, *400*, 213045.

(6) Wu, B.; Tang, D.; Ye, N.; Chen, C. Linear and nonlinear optical properties of the KBe2BO3F2 (KBBF) crystal. *Optical Materials* **1996**, *5*, 105–109.

(7) Maillard, R.; Maillard, A.; Polgár, K. Visible and UV effective non-linear optical coefficients of β-BaB2O4 as function of the growth technique. *Optical Materials* **2009**, *31*, 899–901.

(8) Khan, I.; Kalainathan, S.; Baig, M.; Shkir, M.; Alfaify, S.; Ghramh, H.; Anis, M. Linear-nonlinear optical, dielectric and surface microscopic investigation of KH2PO4 crystal to uncover the decisive impact of dopant glycine. *Materials Science Poland* **2018**, *36*, 662–667.

(9) Delarue, P.; Lecomte, C.; Jannin, M.; Marnier, G.; Menaert, B. Behaviour of the non-linear optical material KTiOPO4 in the temperature range 293-973 K studied by x-ray diffractometry at high resolution: alkaline displacements. *Journal of Physics: Condensed Matter* **1999**, *11*, 4123.

(10) Catella, G. C.; Burlage, D. Crystal growth and optical properties of AgGaS2 and AgGaSe2. *MRS Bulletin* **1998**, *23*, 28–36.

(11) Thomas, P.; Glazer, A.; Watts, B. Crystal structure and nonlinear optical properties of KSnOPO4 and their comparison with KTiOPO4. *Acta Crystallographica Section B: Structural Science* **1990**, *46*, 333–343.

(12) Li, J.-N.; Yao, W.-D.; Li, X.-H.; Liu, W.; Xue, H.-G.; Guo, S.-P. A novel promising infrared nonlinear optical selenide KAg 3 Ga 8 Se 14 designed from benchmark AgGaQ 2 (Q= S, Se). *Chemical Communications* **2021**, *57*, 1109–1112.

(13) Huang, X.; Yang, S.-H.; Li, X.-H.; Liu, W.; Guo, S.-P. Eu2P2S6: The First Rare-Earth Chalcogenophosphate Exhibiting Large Second-Harmonic Generation Response and High Laser-Induced Damage Threshold. *Angewandte Chemie International Edition* **2022**, *61*, e202206791.

(14) Li, J.; Li, X.-H.; Yao, W.-D.; Liu, W.; Guo, S.-P. Three-in-One Strategy Constructing the First High-Performance Nonlinear Optical Sulfide Crystallizing with the P43 Space Group. *Small* **2023**, *19*, 2303090.

(15) Wu, Q.; Kang, L.; Lin, Z. A Machine Learning Study on High Thermal Conductivity

Assisted to Discover Chalcogenides with Balanced Infrared Nonlinear Optical Performance. *Advanced Materials* **2024**, *36*, 2309675.

(16) Li, S.-F.; Jiang, X.-M.; Fan, Y.-H.; Liu, B.-W.; Zeng, H.-Y.; Guo, G.-C. New strategy for designing promising mid-infrared nonlinear optical materials: narrowing the band gap for large nonlinear optical efficiencies and reducing the thermal effect for a high laser-induced damage threshold. *Chemical Science* **2018**, *9*, 5700–5708.

(17) Pasupathi, G.; Philominathan, P. Crystal growth, thermal, optical and microhardness studies of tris (thiourea) magnesium sulphate: a semiorganic nlo material. *Modern Physics Letters B* **2009**, *23*, 3035–3043.

(18) Manivannan, S.; Dhanuskodi, S.; Tiwari, S.; Philip, J. Laser induced surface damage, thermal transport and microhardness studies on certain organic and semiorganic nonlinear optical crystals. *Applied Physics B* **2008**, *90*, 489–496.

(19) Goud, N. R.; Zhang, X.; Bredas, J.-L.; Coropceanu, V.; Matzger, A. J. Discovery of nonlinear optical materials by function-based screening of multi-component solids. *Chem* **2018**, *4*, 150–161.

(20) Chan, E. M. Combinatorial approaches for developing upconverting nanomaterials: high-throughput screening, modeling, and applications. *Chemical Society Reviews* **2015**, *44*, 1653–1679.

(21) Zhang, B.; Zhang, X.; Yu, J.; Wang, Y.; Wu, K.; Lee, M.-H. First-principles high-throughput screening pipeline for nonlinear optical materials: Application to borates. *Chemistry of Materials* **2020**, *32*, 6772–6779.

(22) Kang, L.; Liang, F.; Jiang, X.; Lin, Z.; Chen, C. First-principles design and simulations promote the development of nonlinear optical crystals. *Accounts of Chemical Research* **2019**, *53*, 209–217.

(23) Wang, Z.; Sun, Z.; Yin, H.; Liu, X.; Wang, J.; Zhao, H.; Pang, C. H.; Wu, T.; Li, S.; Yin, Z.; others Data-Driven Materials Innovation and Applications. *Advanced Materials* **2022**, *34*, 2104113.

(24) Hammad, R.; Mondal, S. Predicting Poisson's Ratio: A Study of Semisupervised Anomaly Detection and Supervised Approaches. *ACS omega* **2023**, *9*, 1956–1961.

(25) Zhuo, Y.; Mansouri Tehrani, A.; Brgoch, J. Predicting the band gaps of inorganic solids by machine learning. *The journal of physical chemistry letters* **2018**, *9*, 1668–1673.

(26) Mansouri Tehrani, A.; Oliynyk, A. O.; Parry, M.; Rizvi, Z.; Couper, S.; Lin, F.; Miyagi, L.; Sparks, T. D.; Brgoch, J. Machine learning directed search for ultraincompressible, superhard materials. *Journal of the American Chemical Society* **2018**, *140*, 9844–9853.

(27) Zhang, Z.-Y.; Liu, X.; Shen, L.; Chen, L.; Fang, W.-H. Machine learning with multilevel descriptors for screening of inorganic nonlinear optical crystals. *The Journal of Physical Chemistry C* **2021**, *125*, 25175–25188.

(28) Song, Y.; Lindsay, J.; Zhao, Y.; Nasiri, A.; Louis, S.-Y.; Ling, J.; Hu, M.; Hu, J. Machine learning based prediction of noncentrosymmetric crystal materials. *Computational Materials Science* **2020**, *183*, 109792.

(29) Wang, R.; Liang, F.; Lin, Z. Data-driven prediction of diamond-like infrared nonlinear optical crystals with targeting performances. *Scientific Reports* **2020**, *10*, 3486.

(30) Kresse, G.; Joubert, D. From ultrasoft pseudopotentials to the projector augmented-wave method. *Physical review b* **1999**, *59*, 1758.

(31) Mathew, K.; Montoya, J. H.; Faghaninia, A.; Dwarakanath, S.; Aykol, M.; Tang, H.; Chu, I.-h.; Smidt, T.; Bocklund, B.; Horton, M.; others Atomate: A high-level in-

terface to generate, execute, and analyze computational materials science workflows. *Computational Materials Science* **2017**, *139*, 140–152.

(32) Miller, R. C. Optical second harmonic generation in piezoelectric crystals. *Applied Physics Letters* **1964**, *5*, 17–19.

(33) Jackson, A.; Ohmer, M.; LeClair, S. Relationship of the second order nonlinear optical coefficient to energy gap in inorganic non-centrosymmetric crystals. *Infrared physics & technology* **1997**, *38*, 233–244.

(34) Tripathy, S. Refractive indices of semiconductors from energy gaps. *Optical materials* **2015**, *46*, 240–246.

(35) Moss, T. Relations between the refractive index and energy gap of semiconductors. *physica status solidi (b)* **1985**, *131*, 415–427.

(36) Ravindra, N.; Ganapathy, P.; Choi, J. Energy gap–refractive index relations in semiconductors–An overview. *Infrared physics & technology* **2007**, *50*, 21–29.

(37) Hervé, P.; Vandamme, L. General relation between refractive index and energy gap in semiconductors. *Infrared physics & technology* **1994**, *35*, 609–615.

(38) Reddy, R.; Ahammed, Y. N. A study on the Moss relation. *Infrared physics & technology* **1995**, *36*, 825–830.

(39) Petousis, I.; Chen, W.; Hautier, G.; Graf, T.; Schladt, T. D.; Persson, K. A.; Prinz, F. B. Benchmarking density functional perturbation theory to enable high-throughput screening of materials for dielectric constant and refractive index. *Physical Review B* **2016**, *93*, 115151.

(40) Mazhnik, E.; Oganov, A. R. Application of machine learning methods for predicting new superhard materials. *Journal of Applied Physics* **2020**, *128*.

(41) Chen, X.-Q.; Niu, H.; Li, D.; Li, Y. Modeling hardness of polycrystalline materials and bulk metallic glasses. *Intermetallics* **2011**, *19*, 1275–1281.

(42) Kirklin, S.; Saal, J. E.; Meredig, B.; Thompson, A.; Doak, J. W.; Aykol, M.; Rühl, S.; Wolverton, C. The Open Quantum Materials Database (OQMD): assessing the accuracy of DFT formation energies. *npj Computational Materials* **2015**, *1*, 1–15.

(43) Suceava, A.; Hayden, J.; Kelley, K. P.; Xiong, Y.; Fazlioglu-Yalcin, B.; Dabo, I.; Trolier-McKinstry, S.; Maria, J.-P.; Gopalan, V. Enhancement of second-order optical nonlinearities and nanoscale periodic domain patterning in ferroelectric boron-substituted aluminum nitride thin films. *Optical Materials Express* **2023**, *13*, 1522–1534.